Monitoring General Linear Profiles Using Multivariate Exponentially Weighted Moving Average Schemes

Changliang Zou

LPMC and Department of Statistics
School of Mathematical Sciences
Nankai University
Tianjin, China

Fugee Tsung

Department of Industrial Engineering and
Logistics Management
Hong Kong University of Science and Technology
Clear Water Bay, Kowloon, Hong Kong

Zhaojun Wang

LPMC and Department of Statistics
School of Mathematical Sciences
Nankai University
Tianjin, China

We propose a statistical process control scheme that can be implemented in industrial practice, in which the quality of a process can be characterized by a general linear profile. We start by reviewing the general linear profile model and the existing monitoring methods. Based on this, we propose a novel multivariate exponentially weighted moving average monitoring scheme for such a profile. We introduce two other enhancement features, the variable sampling interval and the parametric diagnostic approach, to further improve the performance of the proposed scheme. Throughout the article, we use a deep reactive ion etching example from semiconductor manufacturing, which has a profile that fits a quadratic polynomial regression model well, to illustrate the implementation of the proposed approach.

KEY WORDS: Change point detection; Linear profiles; Statistical process control.

1. INTRODUCTION

Statistical process control (SPC) has been widely used to monitor various industrial processes. Most SPC applications assume that the quality of a process can be adequately represented by the distribution of a quality characteristic. However, in many situations, the quality of a process may be better characterized and summarized by the relationship between the response variable and one or more explanatory variables; that is, the focus is on monitoring the profile that represents such a relationship instead of on monitoring a single characteristic. Studies focusing on linear profiles have been particularly influential (see, e.g., Jensen, Hui, and Ghare 1984; Mestek, Pavlik, and Suchanek 1994; Stover and Brill 1998; Lawless, Mackay, and Robinson 1999; Kang and Albin 2000).

Kang and Albin (2000) proposed two control charts for phase II monitoring of simple linear profiles, a multivariate T^2 chart and a combination of an exponentially weighted moving average (EWMA) chart to monitor the regression residuals and a range (R) chart to monitor the standard deviations. Kim, Mahmoud, and Woodall (2003) proposed a method based on the combination of three EWMA charts. Instead of using deviations from the in-control (IC) process center, they coded the independent variable so that the average value was 0 and used the estimated regression coefficients from each sample (i.e., the estimates of the Y-intercept and slope) to construct two univariate EWMA charts. They used another one-sided EWMA chart to monitor increases in the standard deviation of the process. Gupta, Montgomery, and Woodall (2006) compared the performance of two phase II monitoring schemes of linear profiles, the control charting schemes proposed by Croarkin and Varner (1982) and Kim et al. (2003). Their simulation study showed that Croarkin and Varner's method performed poorly compared with Kim et al.'s combined control charting scheme. Mahmoud and Woodall (2004) studied the phase I method for monitoring the linear profiles. Following that, Mahmoud, Parker, Woodall, and Hawkins (2007) proposed a changepoint method, based on the likelihood ratio statistics, to detect sustained changes in a linear profile data set in phase I. Zou, Zhang, and Wang (2006) proposed a control chart based on a changepoint model for monitoring linear profiles for which the parameters are unknown but may be estimated from historical samples. An extensive discussion of research problems in monitoring linear profiles has been given by Woodall, Spitzner, Montgomery, and Gupta (2004).

All of these recent studies concentrated on the situation with a simple linear profile that can be adequately represented by a straight line. Although such a simple linear profile can characterize various applications as described in the literature, general linear profiles that include both a polynomial regression and a multiple linear regression relationship may be even more representative of most industrial applications. However, research on monitoring and diagnosis of general linear profiles remains scanty. In this article we focus on studying the phase II method for monitoring a general linear profile that can be represented by a polynomial regression or a multiple linear regression relationship. We propose using a multivariate exponentially weighted moving average (MEWMA) scheme (Lowry,

TECHNOMETRICS, NOVEMBER 2007, VOL. 49, NO. 4
DOI 10.1198/004017007000000164

Woodall, Champ, and Rigdon 1992) for the transformations of estimated parameters as a single chart to monitor both the coefficients and variance of a general linear profile. Different than most of the existing multiple chart approaches, the complexity of the proposed single chart approach will not increase as the profile parameters increase. Also, this chart can be designed and constructed easily and has satisfactory performance. In addition, the proposed MEWMA scheme for general linear profiles can be enhanced by (a) enhancing the proposed charting scheme with variable sampling interval (VSI) features to improve the efficiency of detecting profile changes and (b) providing a systematic diagnostic approach to identify the location of the change and determine which parameters in the profile have changed.

The remainder of the article is organized as follows. In Section 2 we introduce the deep reactive ion etching (DRIE) example from semiconductor manufacturing that motivates this research. We review the general linear profile model and the existing monitoring methods such as those described by Kim et al. (2003) in Section 3. In Section 4 we present our proposed MEWMA schemes. We present the proposed chart with the VSI feature in Section 5, and compare the monitoring performance of the proposed scheme with that of existing methods in Section 6. We provide a systematic approach for profile diagnosis in Section 7, which is critical for a more complicated general linear profile. We also report the performance assessments of the estimates of changepoints and the identification of special causes. We use the motivated DRIE example, which has a profile that fits a quadratic polynomial regression model well, to illustrate the step-by-step implementation of the proposed approach in Section 8. We conclude the article in Section 9 by summarizing its contributions and suggesting some future research. The average run length (ARL) and average time to signal calibrations of the proposed chart, along with several necessary derivations, are given in the Appendix.

2. THE MOTIVATING EXAMPLE: MONITORING A DEEP REACTIVE ION–ETCHING PROCESS

Here we use a microelectromechanical systems (MEMS) fabrication example taken from semiconductor manufacturing to illustrate the motivation for this research. In particular, we select the DRIE process because it is a key operation in MEMS fabrication to form desired patterns on semiconductor wafers and requires careful control and monitoring on a run-to-run basis.

The DRIE process involves complex chemical–mechanical reactions on a machine called an inductively coupled plasma silicon etcher made by Surface Technology Systems Ltd. (See McAuley et al. 2001; Rauf, Dauksher, Clemens, and Smith 2002; Zhou, Zhang, Hao, and Wang 2004 for more details about this system.) The central part of the machine is a process chamber, within which wafers are loaded and processed. The system first releases etching plasma into the chamber to etch trenches following a designed mask pattern; then, in the deposition step, different gases are introduced into the chamber to generate a protective film on the sidewalls. The etching and deposition steps are repeated alternately until a preset processing time is reached or the endpoint detection module confirms the correct etching depth.

In the DRIE process, the quality measurement of an etched wafer is done by scanning electron microscopy in laboratories. One of the most important quality characteristics is the profile of a trench that may significantly impact the downstream operations (May, Huang, and Spanos 1991). The desired profile is the one with smooth and vertical sidewalls, as indicated in center sample of Figure 1; this is called the anisotropic profile. Ideally, the sidewalls of a trench are perpendicular to the bottom of the trench with certain degrees of smoothness around the corners. Various shapes of the profile, such as positive and negative profiles, which are due to underetching and overetching, are considered unacceptable (see Fig. 1).

Current industrial practice is to monitor the angles of the sidewalls. Although the sidewall angle is easier to measure, it is known to contain incomplete information about the trench profile, and in many cases may not differentiate among various out-of-control (OC) profiles. Although it is natural to consider directly monitoring the profile of the trench, which may give more complete information for effective monitoring and diagnosis, exactly how to implement SPC monitoring of a DRIE profile, which apparently cannot be modeled as a straight line, remains a challenge. In the remainder of this article we propose an SPC scheme to monitor such a profile; we give a step-by-step demonstration of how to implement the proposed scheme in practice in a later section.

3. THE GENERAL LINEAR PROFILE MODEL AND EXISTING MONITORING SCHEMES

In this section we describe the modeling of a general linear profile and review the existing profile monitoring schemes in the literature. Assume that for the jth random sample collected over time, we have the observations $(\mathbf{X}_j, \mathbf{Y}_j)$, where $\mathbf{Y}_j$ is n_j-variate vector and $\mathbf{X}_j$ is a $n_j \times p$ $(n_j > p)$ matrix. It is assumed that when the process is in statistical control, the underlying model is

$$\mathbf{Y}_j = \mathbf{X}_j\boldsymbol{\beta} + \varepsilon_j, \tag{1}$$

where $\boldsymbol{\beta} = (\beta^{(1)}, \beta^{(2)}, \ldots, \beta^{(p)})$ is the p-dimensional coefficient vector and the $\boldsymbol{\varepsilon}_j$'s are iid as an n_j-variate multivariate

Figure 1. Various etching profiles from a DRIE process.

normal random vector with mean $\mathbf{0}$ and $\sigma^2\mathbf{I}$ covariance matrix. Without loss of generality, here suppose that $\mathbf{X}_j$ is of form $(\mathbf{1}, \mathbf{X}_j^*)$, where $\mathbf{X}_j^*$ is orthogonal to $\mathbf{1}$ and $\mathbf{1}$ is a n_j-variate vector of all 1's. Otherwise, we can obtain this form through some appropriate transformations. The n_j's are usually equal (denoted as n) and the explanatory variable, $\mathbf{X}_j$, is assumed to be fixed for different j (denoted as $\mathbf{X}$). This is usually the case in practical calibration applications and is also consistent with the work of Kang and Albin (2000), Kim et al. (2003), and Mahmoud and Woodall (2004), where the emphasis is on simple linear regression. Woodall et al. (2004) also mentioned the extension of simple linear profiles to other, more complex linear profiles and listed some relevant references. Jensen et al. (1984) also studied this profile, although their model is not exactly the same. Their schemes are similar to those of Kim et al. (2003) but focus on controlling one parameter of the coefficients and variance individually. They proposed some Shewhart-type control charts for monitoring the coefficients and variance.

The simplest case of model (1), the straight-line regression model, was considered by Kang and Albin (2000), Kim et al. (2003), Mahmoud and Woodall (2004), and Mahmoud et al. (2007). Denote by $\{(x_i, y_{ij}), i = 1, 2, \ldots, n\}$ the jth random sample collected over time. When the process is in control, the relationship between the response and explanatory variables is assumed to be

$$y_{ij} = A_0 + A_1 x_i + \varepsilon_{ij}, \qquad i = 1, 2, \ldots, n, \tag{2}$$

where the ε_{ij}s are iid normal random variables with mean 0 and variance σ^2.

Using the coded explanatory values, Kim et al. (2003) obtained the following alternative form of the underlying model:

$$y_{ij} = B_0 + B_1 x_i^* + \varepsilon_{ij}, \qquad i = 1, 2, \ldots, n, \tag{3}$$

where $B_0 = A_0 + A_1\bar{x}$, $B_1 = A_1$, $x_i^* = (x_i - \bar{x})$, and $\bar{x} = \frac{1}{n}\sum_{i=1}^n x_i$. For the jth sample, the least squares estimators for B_0, B_1, and σ^2 are

$$b_{0j} = \bar{y}_j, \qquad b_{1j} = \frac{S_{xy(j)}}{S_{xx}}, \qquad \text{and}$$
$$MSE_j = \frac{1}{n-2}\sum_{i=1}^{n}(y_{ij} - b_{1j}x_i^* - b_{0j})^2, \tag{4}$$

where $\bar{y}_j = \frac{1}{n}\sum_{i=1}^n y_{ij}$, $S_{xx} = \sum_{i=1}^n (x_i - \bar{x})^2$, and $S_{xy(j)} = \sum_{i=1}^n (x_i - \bar{x})y_{ij}$. Note that these three estimators are independent. Thus they proposed using three EWMA charts (EWMA_I, EWMA_S, and EWMA_E) to detect whether the Y-intercept (B_0), slope (B_1), and standard deviation (σ) had changed:

$$\text{EWMA}_I(j) = \theta b_{0j} + (1-\theta)\text{EWMA}_I(j-1),$$
$$\text{EWMA}_S(j) = \theta b_{1j} + (1-\theta)\text{EWMA}_S(j-1),$$

and

$$\text{EWMA}_E(j) = \max\{\theta \ln(MSE_j) + (1-\theta)\text{EWMA}_E(j-1), \ln(\sigma^2)\},$$

where $\text{EWMA}_I(0) = B_0$, $\text{EWMA}_S(0) = B_1$, $\text{EWMA}_E(0) = \ln(\sigma^2)$, and θ is a smoothing constant. The three EWMA charts are used jointly, and the profile change is detected as one of the chart signals. Their ARL comparisons show that the three EWMA charts are more effective than the method of Kang and Albin (2000) in terms of detecting sustained shifts in the Y-intercept and slope and increases in the error variance. The three EWMA charts are particularly effective in detecting shifts in the slope of the line, that is, the changes in parameter B_1 of (3). Also, the authors argued that their method seemed more interpretable. Thus, in this article we use the combined MEWMA charts approach (designated the KMW chart hereinafter) as a benchmark for comparisons with our proposed scheme.

Note that monitoring simple linear profiles that have three parameters to be controlled is similar to monitoring the two parameters of mean (μ) and variability (σ^2) simultaneously in conventional SPC applications. The combination of two EWMA charts is usually required to monitor both the mean and variability. Gan (1995) suggested a simple procedure for designing a combination using a two-sided EWMA chart for the mean and two one-sided EWMA charts for the variability. His method is similar to the approach of Kim et al. (2003). One difference is the number of the parameters to be controlled; another is that Kim et al. (2003) considered only the upper-sided chart for detecting the standard deviation. Reynolds and Stoumbos (2001) also considered using two EWMA charts for individual observations.

As we can see, the KMW approach requires three EWMA charts (with another one-sided EWMA chart possibly needed to detect a decrease in variance) to be handled side by side, each one having a statistic that must be updated and plotted for every sample. Such a scheme may be manageable for a simple linear profile case, but it can become quite complicated and infeasible for a general linear profile, because the setup of general profile charting schemes requires that even more control charts be combined simultaneously to monitor these additional parameters. Thus the design, implementation, and performance assessment of such a combined scheme will be rather complex and impractical.

In this article we propose using a single chart to monitor all of the profile parameters so that the design and operation of the monitoring scheme can be greatly simplified. Here we consider the phase II case in which the IC values of parameters $\boldsymbol{\beta}$ and σ^2 are assumed to be known; that is, it is assumed that the IC data set used in phase I is large enough so that errors associated with estimating the three parameters can be neglected.

4. A NOVEL MULTIVARIATE EXPONENTIALLY WEIGHTED MOVING AVERAGE CHART FOR MONITORING A GENERAL LINEAR PROFILE

In this section we propose a novel MEWMA scheme to monitor a general linear profile. When monitoring a general linear profile model (1), $p+1$ parameters, p coefficients, and the standard deviations σ must be controlled simultaneously. Following the notation in model (1), we define

$$\mathbf{Z}_j(\boldsymbol{\beta}) = (\widehat{\boldsymbol{\beta}}_j - \boldsymbol{\beta})/\sigma \tag{5}$$

and

$$Z_j(\sigma) = \Phi^{-1}\{F((n-p)\widehat{\sigma}_j^2/\sigma^2; n-p)\}, \tag{6}$$

where $\widehat{\boldsymbol{\beta}}_j = (\mathbf{X}'\mathbf{X})^{-1}\mathbf{X}'\mathbf{Y}_j$, $\widehat{\sigma}_j^2 = \frac{1}{n-p}(\mathbf{Y}_j - \mathbf{X}\widehat{\boldsymbol{\beta}}_j)'(\mathbf{Y}_j - \mathbf{X}\widehat{\boldsymbol{\beta}}_j)$, $\Phi^{-1}(\cdot)$ is the inverse of the standard normal cumulative distribution function, and $F(\cdot;\nu)$ is the chi-squared distribution function with ν degrees of freedom (χ^2_ν). Note that this type of variance transformation with the use of an EWMA chart have been suggested by Quesenberry (1995) and Chen, Cheng, and Xie (2001). Such a transformation has fairly nice properties; the distribution of $Z_j(\sigma)$ is independent of the sample size, n, when the process is in control, and thus we can handle the case of variable sample size conveniently. Moreover, the choice of the control limits will not be affected by n, so that the control chart can be designed more easily. Another advantage of transforming $\widehat{\sigma}_j^2$ to $Z_j(\sigma)$ is that the distribution of $Z_j(\sigma)$ will be symmetric, so that the control chart can be sensitive to decreases in the standard deviation as well. Denote $\mathbf{Z}_j$ by $(\mathbf{Z}_j'(\beta), Z_j(\sigma))'$, which is a $(p+1)$-variate random vector. When the process is in control, the vector is multivariate normally distributed with mean 0 and covariance matrix $\boldsymbol{\Sigma} = \begin{pmatrix} (\mathbf{X}'\mathbf{X})^{-1} & \mathbf{0} \\ \mathbf{0} & 1 \end{pmatrix}$.

Here the EWMA charting statistic is defined as

$$\mathbf{W}_j = \lambda\mathbf{Z}_j + (1-\lambda)\mathbf{W}_{j-1}, \qquad j = 1, 2, \ldots, \tag{7}$$

where $\mathbf{W}_0$ is a $(p+1)$-dimensional starting vector and λ is a parameter (chosen such that $0 < \lambda \leq 1$) that regulates the magnitude of the smoothing. The chart signals are

$$U_j = \mathbf{W}_j'\boldsymbol{\Sigma}^{-1}\mathbf{W}_j > L\frac{\lambda}{2-\lambda}, \tag{8}$$

where $L > 0$ is chosen to achieve a specified IC ARL. This control scheme can be deemed a special application of MEWMA charts. The MEWMA chart was first proposed by Lowry et al. (1992); the design of MEWMA charts was investigated by Prabhu and Runger (1997).

In this article the smoothing constant, λ, in (7) is first taken to be .2 in our numerical study, which is consistent with the approach of Kim et al. (2003). In general, a smaller λ leads to more rapid detection of smaller shifts (Lucas and Saccucci 1990; Prabhu and Runger 1997). The starting vector, $\mathbf{W}_0$, is chosen to be the zero vector, and the control limits, L, are fixed according to the designed IC ARL and λ.

Through the transformation, the control limits of the proposed MEWMA chart are independent of size, n. Therefore, the control limits, L, can be conveniently obtained for various values of p and λ. A computer program for determining L, is available from on request.

In this article we evaluate the charting performance by ARL. Runger and Prabhu (1996) and Rigdon (1995a,b) presented theoretical developments with Markov chains and integral equations, to determine the performance of MEWMA charts. Here we extend the work of Runger and Prabhu (1996) and easily calculate the IC and OC ARL of the proposed MEWMA chart through the Markov chain model. The details are presented in the Appendix. Kim et al. (2003) analyzed the performance of their KMW chart through simulations. The control limits of the three EWMA charts are chosen so that each individual chart has the same IC ARL, while jointly achieving a specified overall IC ARL. The determination of control limits for the KMW chart by simulation is not trivial, because large numbers of simulated runs are required to obtain an acceptable standard error. Moreover, because the control limits of the KMW chart also depend on the sample size, n, the design of this scheme could be tedious. Although a three-dimensional Markov chain may be explored to evaluate the performance of the KMW chart, there would be a considerable computational burden.

Kang and Albin (2000) proposed an alternative using the T^2 chart, which is also a single multivariate chart that monitors a profile. The T^2 chart is a Shewhart-type multivariate chart, whereas our proposed chart is a EWMA-type chart. In addition to the difference in chart type, we use a random vector with mean 0 and covariance matrix $\boldsymbol{\Sigma}$ that contains the transformation of the standard deviation, whereas Kang and Albin's T^2 chart does not. The resulting advantage is that our proposed chart would be effective in detecting both the increase and decrease in the standard deviation and sensitive to small and moderate shifts as well.

Another alternative that also may be applied to the linear profile case is the MaxEWMA chart proposed by Chen et al. (2001). This chart monitors the maximum absolute value of $\mathbf{DW}_j$'s $p+1$ components instead of U_j, where the matrix $\mathbf{D}$ is a $(p+1)$-dimensional matrix, so that $\mathbf{DZ}_j$ becomes a standard multivariate normal vector when the process is in control. The MaxEWMA chart can be viewed as an integration of EWMA procedures and a generalized likelihood ratio for testing the change in only one component of the standard multivariate normal vector, whereas the MEWMA chart combines the EWMA scheme with the traditional Hotelling T^2 (chi-squared when covariance matrix is known) test. Thus we may expect the MaxEWMA approach to outperform the MEWMA chart when indeed only a single component of $\mathbf{DZ}_j$ shifts, whereas the MEWMA chart may have better performance when several components shift simultaneously. Performance comparisons of these two control schemes have been conducted (available on request), and numerical results demonstrate this claim. However, as one referee pointed out, compared with the MaxEWMA chart, a special good characteristic of the MEWMA chart is its affine-invariant property whenever the process is in control or out of control.

Note that there are many possible choices for the matrix $\mathbf{D}$ for constructing the MaxEWMA chart. The OC performance of the MaxEWMA scheme strongly depends on the choice of $\mathbf{D}$, although the IC distribution of $\mathbf{DZ}_j$ is the same. For the considered general linear profile problem, in practice, we usually cannot anticipate which coefficient or combination of coefficients in model (1) may change. Therefore, it is difficult to give a "good" matrix $\mathbf{D}$ that corresponds to the accurate direction of shift before we start monitoring. Moreover, similar to the drawback of the KMW chart, the performance of the MaxEWMA chart is difficult to evaluate, because this must be done through simulations. Although Calzada, Scariano, and Chen (2004) used a two-dimensional integral equation to obtain the ARLs for the chart proposed by Chen et al. (2001), extending this method to even the three-dimensional case would require an excessive computational load.

Another concern mentioned by Kim et al. (2003) and Woodall et al. (2004) is that although the MEWMA chart may improve the performance of the T^2 chart, the interpretation of an out-of-control signal would not be straightforward. In Section 7 we propose a simple diagnostic aid that can provide information for identifying and isolating the out-of-control signal with at least comparable diagnostic performance to that of the KMW scheme.

5. ADDING VARIABLE SAMPLING FEATURES TO THE PROPOSED PROFILE MONITORING SCHEME

The VSI scheme is a known approach to enhancing the efficiency of SPC monitoring schemes. However, existing multiple chart profile monitoring schemes, such as the KMW scheme, cannot readily incorporate the VSI feature. Because MEWMA is a single chart, a VSI version can be designed and implemented for a general linear profile without much modification and can largely improve the efficiency in detecting profile changes.

The conventional practice in applying SPC control charts to monitoring a process is to use a fixed sampling rate (FSR) that takes samples of fixed sample size (FSS) at a fixed sampling interval (FSI). In recent years, several modifications have been suggested to improve traditional FSR policies that provide better performance than conventional charts in the sense of quicker responses to a process change. Among these, adopting a variable sampling interval in a control chart instead of a FSI is one of the most popular and useful approaches to improving the detection ability. In a VSI control chart, the sampling interval is varied as a function of the control statistic. The basic idea of the VSI feature is to use a shorter sampling interval if there is an indication of a possible change, but a longer sampling interval if there is no such indication.

Many researchers have contributed to the theory and practice of the VSI chart. Most work on developing VSI control charts focuses on monitoring the mean (e.g., Reynolds, Amin, Arnold, and Nachlas 1988; Reynolds 1989; Reynolds, Amin, and Arnold 1990; Runger and Montgomery 1993; Reynolds and Arnold 2001). Chengular, Arnold, and Reynolds (1989) introduced a VSI Shewhart chart for monitoring the mean and variance with a sample size of $n > 1$. Reynolds and Stoumbos (2001) added the VSI feature to various combinations of control charts to detect the shift in the mean and variance using individual observations. There are few research works on VSI multivariate control charts. Aparisi (2001) considered a VSI control chart based on Hotelling's statistic. Reynolds and Kim (2005a,b) recently investigated MEWMA control charts based on sequential sampling and unequal sample sizes.

Past work on VSI control charts (see, e.g., Reynolds 1989) has shown that using only two possible values for the sampling intervals is sufficient. Thus, in this article we consider two possible interval values, say $0 < d_1 \le d_2$. To apply the VSI feature to the MEWMA control chart, we apply additional warning limits $0 \le L_1 \le L$ inside the control limits to determine which sampling interval to use next. In particular, a long sampling interval, d_2, should be used after the sample, j, is obtained if U_j falls inside the warning limits of $L_1\frac{\lambda}{2-\lambda}$. On the other hand, a short sampling interval, d_1, should be used if U_j falls outside of these limits but inside the control limits of $L\frac{\lambda}{2-\lambda}$. If U_j falls outside of the control limits, then an out-of-control signal would be triggered, as in the case of the traditional FSI MEWMA chart.

When evaluating the statistical performance of a VSI control chart, both the average time to signal (ATS) and average number of samples to signal (ANSS) should be considered, because the ATS is not simply a constant multiple of the ANSS, as is the case with an FSI chart. In the comparative study in this article, we require that all of the charts being compared have the same in-control sampling rate and the same false-alarm rate. This ensures that the charts being compared will have the same ATS and ANSS when the process is in control. When different control charts being compared are designed to have the same IC ATS and ANSS, these charts then can be fairly compared according to the steady-state ATS (SSATS). The SSATS is defined as the expected time from the point of the shift to the point at which the chart signals, under the assumption that the control statistic has reached a stationary or steady-state distribution by the time that the shift occurs.

The assumptions used in defining the SSATS have been discussed by Reynolds et al. (1990). Computation of SSATS is more complicated than that of ATS, because the point at which the shift occurs may fall within the interval between two samples. For the VSI and FSI MEWMA charts, the ATS and SSATS also can be evaluated by the Markov chain approximation, which is detailed in the Appendix. Performance comparisons of FSI and VSI schemes are presented in Section 6.

6. MONITORING PERFORMANCE COMPARISONS

In this section we investigate the monitoring performance of the proposed MEWMA scheme through ARL comparisons. Although our proposed control chart can be used to monitor the general linear profile model (1), there seem to be no other effective and comparable methods for such a model except for the simple straight-line model (2), that is, $p = 2$ in model (1). Thus we compare the performance of our proposed control chart and the KMW chart under model (2) [or, equivalently, (3)].

For simplicity and consistency with the literature, we assume the changepoint to be $\tau = 0$ and considered only the case of overall IC ARL = 200. The underlying IC model is the same as that of Kang and Albin (2000), in which the parameters in the in control model are $A_0 = 3, A_1 = 2, \sigma^2 = 1$, and $x_i = 2, 4, 6, 8$. Kim et al. (2003) set the control limits to be 3.0156, 3.0109, and 1.3723 for the three EWMA charts ($EWMA_I$, $EWMA_S$, and $EWMA_E$) when the smoothing constant, λ, is chosen to be .2. In the case of known parameters, this design has an overall IC ARL of roughly 200, and the IC ARL of each chart is about 584. The ARL results of the KMW and MEWMA charts are evaluated with 50,000 simulations and Markov chain approximation. Moreover, the types of shifts considered in this article are consistent with those of Kim et al. (2003).

We compared our proposed MEWMA chart with the KMW chart in terms of out-of-control ARL. The OC ARLs of our MEWMA chart and that of the KMW chart for detecting shifts in A_0, A_1, σ, and B_1 are given in Table 1. Note that when the process parameter A_1 is changed to $A_1 + \delta_1\sigma$, it can be easily checked that the noncentrality parameter, δ, in (A.1) of the Appendix becomes $\delta_1\sqrt{n \cdot \bar{\tilde{X}} + S_{xx}}$. This table shows that for detecting any shift in A_1, the two charts have very similar performance with large shifts. With small and moderate shifts, our proposed MEWMA performs little better than the KMW chart. Also, for detecting a shift in the standard deviation, our proposed MEWMA chart performs better than the KMW chart, but with a very small shift. Our proposed MEWMA chart has a slight disadvantage in detecting the moderate and large shifts in intercepts A_0 and B_1 compared with the KMW chart, but the difference between them seems negligible.

Table 1. ARL comparisons between MEWMA and KMW charts for shifts in A_0, A_1, the standard deviation, and B_1

A_0			A_1			σ			B_1		
δ_1	MEWMA	KMW	δ_1	MEWMA	KMW	δ_1	MEWMA	KMW	δ_1	MEWMA	KMW
.1000	131.5	133.7	.0250	99.0	101.6	1.1000	76.2	72.8	.0500	120.5	120.8
.2000	59.9	59.1	.0375	57.4	61.0	1.1500	48.7	48.1	.0750	77.3	77.3
.3000	29.6	28.3	.0500	35.0	36.5	1.2000	33.2	33.5	.1000	50.0	49.1
.4000	17.2	16.2	.0625	23.1	24.6	1.2500	24.1	24.9	.1500	24.0	22.8
.5000	11.5	10.7	.0750	16.4	17.0	1.3000	18.4	19.4	.2000	14.0	13.1
.6000	8.5	7.9	.1000	9.8	10.3	1.4000	12.1	12.7	.2500	9.5	8.9
.8000	5.8	5.1	.1250	6.9	7.2	1.6000	7.0	7.2	.3000	7.1	6.6
1.0000	4.1	3.8	.1500	5.3	5.5	1.8000	4.9	5.1	.4000	4.7	4.4
1.5000	2.6	2.4	.2000	3.7	3.8	2.2000	3.1	3.2	.5000	3.6	3.3
2.0000	2.0	1.9	.2500	2.9	2.9	2.6000	2.3	2.5	.7000	2.5	2.3
						3.0000	1.9	2.1	.9000	2.0	1.9

Note that in detecting the change of the standard deviation, the KMW chart is an upper-sided scheme; that is, it is for detecting an increase but not directly for detecting a decrease in variance. However, our approach can detect the decreases in variance without modification. The ARL results are given in Table 2.

Simultaneous shifts in the intercept and slope in model (3) are also considered in this article. The OC ARL values are obtained and summarized in Table 3. The magnitudes of shifts in intercept (B_0) δ_1 and slope (B_1) δ_2 are consistent with Kim et al. (2003). It can be clearly seen that the noncentrality parameter is $\delta = \sqrt{\delta_1^2 n + \delta_2^2 S_{xx}}$. Here the MEWMA chart performs better than the KMW chart in most cases except when one of δ_1 and δ_2 is very large and the other is very small.

We may conclude from Tables 1–3 that for detecting shifts in simple linear profiles, the single-scheme MEWMA chart has at least comparable performance to the combination-scheme KMW chart. The MEWMA chart usually outperforms the KMW chart when several parameters have changed. Other numerical results have been obtained (available on request) for shifts in combinations of either B_0 and σ or B_1 and σ to validate this argument.

Finally, we demonstrate the improved performance gained in terms of ATS by adding the VSI feature to the MEWMA chart for monitoring linear profiles. Although the VSI feature also may be applied to the KMW chart, the design of the combination of three VSI EMWA charts is not at all trivial, because three warning limits and three control limits must be chosen simultaneously so that all charts have the same individual IC average sampling rate and IC average false-alarm rate. Here we compare only the SSATS of the FSI and VSI MEWMA charts. We do not tabulate the SSATS of the FSI KMW chart, because the performance of the KMW chart would be similar to that of the MEWMA chart. Table 4 presents the SSATS values of the VSI and FSI MEWMA charts for the linear profiles models (2). The shifts in intercept and standard deviation are investigated. The IC ATS and ANSS of each chart are both set to 200; that is, the average IC sampling rate of the VSI chart is 1 sample per unit time. All of the numerical results given in Table 4 were obtained by Markov chain approximation.

From Table 4, we conclude that adding the VSI feature can provide quite substantial reductions in the time required to detect small and moderate shifts. The results presented here are fairly consistent with previous research on univariate VSI control charts. In general, the interval, d_1, should be as small as possible for better statistical performance (Reynolds et al. 1990); therefore, it usually depends on how soon that it is feasible to sample again after the current sample was obtained. On the other hand, the sampling interval d_2 could be chosen to be long so that the resulting control chart would have an acceptable

Table 2. ARLs of the MEWMA chart in detecting a decrease in variance

δ_1	.10	.15	.20	.25	.30	.35	.40
ARL	3.3	3.9	4.5	5.3	6.4	7.8	9.7
δ_1	.45	.50	.55	.60	.65	.70	.75
ARL	12.5	16.5	22.9	33.0	49.1	74.9	114.5

Table 3. ARL comparisons between MEWMA and KMW charts under combinations of intercept (δ_1) and slope (δ_2) shifts in model (3)

	MEWMA	δ_2									
	KMW	.025	.050	.075	.100	.125	.150	.175	.200	.225	.250
δ_1	.05	155.8	111.0	72.9	48.0	32.8	23.5	17.7	13.9	11.3	9.5
		157.6	114.7	74.8	48.3	32.2	22.5	16.9	13.2	10.7	8.9
	.10	118.0	89.2	62.1	42.8	30.2	22.2	16.9	13.5	11.0	9.3
		122.1	94.6	66.4	44.9	30.7	21.9	16.6	13.1	10.6	8.9
	.15	82.2	66.3	49.5	36.1	26.7	20.2	15.8	12.8	10.6	9.0
		84.6	70.8	54.5	39.6	28.5	20.9	16.1	12.8	10.4	8.8
	.20	56.4	48.0	38.2	29.6	22.9	18.1	14.5	12.0	10.1	8.7
		57.1	51.1	42.4	33.3	25.4	19.5	15.4	12.4	10.2	8.7
	.25	39.5	35.0	29.4	24.0	19.5	15.9	13.2	11.1	9.5	8.2
		39.5	36.5	32.3	27.1	22.0	17.8	14.4	11.9	10.0	8.5
	.30	28.7	26.2	22.9	19.6	16.5	13.9	11.8	10.2	8.8	7.8
		28.2	26.9	24.7	22.0	18.8	15.7	13.2	11.2	9.6	8.3
	.35	21.7	20.2	18.3	16.1	14.0	12.2	10.6	9.3	8.2	7.3
		20.9	20.2	19.1	17.6	15.8	13.9	12.1	10.5	9.1	8.0
	.40	17.0	16.1	14.9	13.5	12.0	10.7	9.5	8.5	7.6	6.9
		16.2	15.9	15.3	14.5	13.5	12.1	10.9	9.7	8.6	7.6
	.45	13.7	13.2	12.4	11.4	10.5	9.5	8.6	7.8	7.1	6.5
		13.1	12.9	12.6	12.1	11.4	10.6	9.8	8.9	8.0	7.3
	.50	11.4	11.1	10.5	9.9	9.2	8.5	7.8	7.2	6.6	6.1
		10.8	10.8	10.6	10.3	9.9	9.3	8.7	8.1	7.5	6.9

Table 4. SSATS comparisons between FSI MEMWA and VSI MEWMA charts for the shift in intercept and standard deviation

	A_0					σ			
		VSI					VSI		
δ_1	FSI	$d_1 = .5$ $d_2 = 1.25$	$d_1 = .25$ $d_2 = 1.5$	$d_1 = .1$ $d_2 = 1.9$	δ_1	FSI	$d_1 = .5$ $d_2 = 1.25$	$d_1 = .25$ $d_2 = 1.5$	$d_1 = .1$ $d_2 = 1.9$
.1	127.9	124.4	122.2	120.0	.1	2.7	2.1	1.9	1.8
.2	57.6	51.9	48.3	45.2	.3	5.8	4.3	3.6	3.3
.4	28.1	23.3	20.4	18.1	.5	15.9	11.2	8.7	7.1
.4	16.1	12.6	10.6	9.2	.7	73.8	63.9	57.6	51.1
.5	10.6	8.0	6.6	5.8	1.1	73.2	68.9	66.3	63.9
.6	7.6	5.7	4.8	4.2	1.2	31.2	27.4	25.2	23.4
.8	4.8	3.6	3.1	2.8	1.4	16.9	14.1	12.5	11.4
1.0	3.4	2.6	2.3	2.1	1.8	10.8	8.8	7.7	6.9
1.5	2.0	1.6	1.4	1.4	2.2	4.0	3.2	2.7	2.6
2.0	1.4	1.1	1.0	1.1	2.6	2.4	1.9	1.7	1.7
3.0	.8	.7	.8	.9	3.0	1.3	1.1	1.1	1.2

average sampling rate. Similar conclusions can be obtained for other types of changes as well.

7. DIAGNOSTIC AIDS IN PROFILE MONITORING

In the practice of quality control, along with detecting a process change quickly, it is also critical to diagnose the change and identify which parameter or parameters in a profile have shifted after an out-of-control signal occurred. Such a diagnosis is particularly important in general linear profile monitoring, where there more process parameters are involved. A diagnostic aid to locate the changepoint in the process and to isolate the type of parameter change in a profile will help an engineer identify and eliminate the root cause of a problem quickly and easily. In this section we discuss the diagnosis of a general linear profile and provide a systematic diagnostic approach to identify the location of the change and which parameters in the profile that have changed.

7.1 Estimate of the Changepoint in Profile Monitoring

To identify the location of a changepoint in profile monitoring, a maximum likelihood estimator (MLE) of the changepoint statistic is used. We assume that an out-of-control signal is triggered at subgroup k by the MEWMA chart. Our suggested estimator of the changepoint, τ, of a step shift is given by

$$\hat{\tau} = \arg\max_{0 \le t < k} \{lr(tn, kn)\}, \tag{9}$$

where $lr(tn, kn)$ is the generalized likelihood ratio statistic. The expressions of $lr(tn, kn)$ and the involved deductions are given in the Appendix. This estimator has been used for offline nonsequential changepoint detection in linear models in the literature (see Csorgo and Horvath 1997, chap. 3, for more details). In this article we use it in an online SPC application. Zou et al. (2006) recently suggested a similar estimator, using a standardized generalized likelihood ratio statistic instead, when the true parameters of the linear profile are unknown. Note that Nishina (1992) proposed an estimator for the process changepoint when a traditional EWMA control chart sends out a signal. Pignatiello and Samuel (2001) showed that the MLE method performs much better than the method proposed by Nishina (1992) for a conventional process change. Because we believe that this result should be valid for the linear profile model as well, we do not investigate Nishina's (1992) method further in this article.

Here we conduct simulations to evaluate the effectiveness of the estimator (9). In the simulations, we used the changepoint $\tau = 100$. We generated 50,000 independent series in the simulations. Any series in which a signal occurs before the $\tau + 1$ product observations was discarded. Table 5 tabulates the average (AVE) and standard deviation (SD) of the estimate $\hat{\tau}$ for the shift in intercept and variance under model (3). In also presents the observed frequencies with which the estimator are within a given number of samples around the actual τ, that is, the probabilities $\Pr(\hat{\tau} = \tau)$, $\Pr(|\hat{\tau} - \tau| \le 1)$, $\Pr(|\hat{\tau} - \tau| \le 3)$, and $\Pr(|\hat{\tau} - \tau| \le 5)$ (denoted by P_0, P_1, P_3, and P_5 in Table 5). These probabilities may provide certain indications of the precision of the estimator.

Table 5. The average (AVE), standard deviation (SD), and precision of changepoint estimates for the proposed method

	B_0						σ						
δ_1	AVE	SD	P_0	P_1	P_3	P_5	δ_1	AVE	SD	P_0	P_1	P_3	P_5
.4	102.6	13.3	.13	.27	.45	.58	1.4	100.5	10.5	.20	.39	.60	.73
.8	99.6	7.0	.40	.63	.83	.91	1.8	99.6	6.2	.45	.69	.87	.93
1.2	99.6	4.7	.63	.83	.94	.97	2.2	99.6	4.9	.61	.83	.94	.97
1.6	99.8	2.6	.79	.94	.98	.99	2.6	99.7	3.5	.72	.90	.97	.98
2.0	99.8	2.3	.89	.97	.98	.99	3.0	99.8	2.6	.79	.94	.98	.99

Table 5 shows that the proposed estimator performs well from the standpoint of the average for any shift size. We can also see that $\hat{\tau}$ has better precision as the magnitude of the shift increases. These findings on the MLE for profile monitoring are consistent with Pignatiello and Samuel's (2001) conclusion on conventional nonprofile monitoring.

7.2 Identification of the Out-of-Control Profile Parameters

After locating the changepoint in a profile, it is also critical to identify the specific parameter in the profile that has changed. Because the proposed chart of Kim et al. (2003) is a combination of three EWMA charts and each chart detects the corresponding parameter, the diagnosis of any process change is easier than that of omnibus methods of Kang and Albin (2000). However, there is also a drawback in using the combination of charts to determine which parameter has changed. When one of the charts has signaled, engineers will usually go only after that specific charting parameter and ignore the possibility that there may be other parameters that have changed as well. In addition, using combination schemes such as the KMW chart to diagnose a special cause may not be appropriate for a general linear profile, because the components of $\hat{\boldsymbol{\beta}}$ are usually correlated except in a simple linear profile.

At a first glance, our proposed method based on a single chart seems to be unable to diagnose which parameter has changed. However, as Reynolds and Stoumbos (2005) pointed out, the control charts used as diagnostic aids do not necessarily have to be the same control charts used to determine when to signal. Similar arguments were also given by Hawkins and Zamba (2005), who used two parametric tests to determine whether the shift comes from the mean or from the variance. Consequently, in this article we propose using a parametric test method as an auxiliary tool to determine which parameters in a profile that have changed after the chart has triggered a signal. Write

$$\tilde{\boldsymbol{\beta}}_{t,k} = \frac{1}{k-t}(\mathbf{X}'\mathbf{X})^{-1}\mathbf{X}' \sum_{j=t+1}^{k} \mathbf{Y}_j \tag{10}$$

and

$$\tilde{\sigma}^2_{t,k} = \frac{1}{(k-t)n-p} \sum_{j=t+1}^{k} (\mathbf{Y}_j - \mathbf{X}\tilde{\boldsymbol{\beta}}_{t,k})'(\mathbf{Y}_j - \mathbf{X}\tilde{\boldsymbol{\beta}}_{t,k}). \tag{11}$$

Assume that the MEWMA chart signaled at kth sample, after obtaining the change point estimator $\hat{\tau}$ using (9). The tests for the Y-intercept, standard deviation, and regression coefficients are as follows. We use the t-test for a Y-intercept change using $(k-\hat{\tau})n-p$ degrees of freedom and the test statistic

$$T_{test} = \frac{\sqrt{(k-\hat{\tau})n}(\tilde{\beta}^{(1)}_{\hat{\tau},k} - \beta^{(1)})}{\tilde{\sigma}_{\hat{\tau},k}}, \tag{12}$$

where $\tilde{\beta}^{(1)}_{\hat{\tau},k}$ denotes the first component of the p-dimensional vector, $\tilde{\boldsymbol{\beta}}_{\hat{\tau},k}$. Also, the chi-squared test is used for a standard deviation change using $(k-\hat{\tau})n-p$ degrees of freedom and the test statistic

$$\chi^2_{test} = \frac{[(k-\hat{\tau})n-p]\tilde{\sigma}^2_{\hat{\tau},k}}{\sigma^2}. \tag{13}$$

For the rest of the $p-1$ profile parameters $(\beta^{(2)},\ldots,\beta^{(p)})$, by considering the correlations between their estimators, we follow the work of Jensen et al. (1984) and use the following test with a rejection region:

$$F^{(i)}_{test}: \quad (k-\hat{\tau})\big(\tilde{\beta}^{(i)}_{\hat{\tau},k} - \beta^{(i)}\big)^2/m_{ii}\tilde{\sigma}^2_{\hat{\tau},k} > F_\alpha\big(p-1,(k-\hat{\tau})n-p,\mathbf{R}\big) \tag{14}$$

for each $i=2,\ldots,p$, where the m_{ii}'s are diagonal elements of $\mathbf{M}=(\mathbf{X}'\mathbf{X})^{-1}$, $\mathbf{R}=\operatorname{diag}\{m_{11}^{-1/2},\ldots,m_{pp}^{-1/2}\}\mathbf{M}\operatorname{diag}\{m_{11}^{-1/2},\ldots,m_{pp}^{-1/2}\}$, is the correlation matrix for $\hat{\boldsymbol{\beta}}$, and $F_\alpha(p-1,(k-\hat{\tau})n-p,\mathbf{R})$ is the upper α percentile of the multivariate F distribution with parameters $(p-1,(k-\hat{\tau})n-p,\mathbf{R})$ (see Kotz, Balakrishnan, and Johnson 2000).

Here we compare the diagnostic ability of indicating out-of-control parameters between the foregoing hypothesis test method with $\alpha=.05$ and the KMW chart under a simple linear model (3). The simulation results are tabulated in Table 6.

In this table, three digits in the first row present various combinations of parameter changes in the Y-intercept, slope, and standard deviation. For example, the three digits in "100" correspond to the Y-intercept, slope, and standard deviation, in which the first digit, "1," means a change in the Y-intercept and the second and third digits, "00," mean no shift in the other two parameters. The simulated estimates of the probabilities of events occurring at "100," "010," and so on for various shift patterns are presented, where the upper and lower entries are obtained by the KMW chart and the parametric tests. These probabilities indicate the accuracies of the diagnostic approaches, with larger values indicating a greater diagnostic accuracy.

Table 6. Comparison of diagnostic abilities of the method using the KMW chart and parametric test for shifts in B_0, B_1, and standard deviation in model (3)

δ_I	δ_S	δ_σ	100	010	001	110	101	011	111
.4	0	1.0	.942	.029	.027	.001	.002	0	.001
			.652	.024	.020	.136	.081	.005	.062
.8	0	1.0	.979	.011	.008	.002	.001	0	0
			.746	.008	.013	.105	.069	.001	.039
0	.10	1.0	.079	.839	.079	.001	.001	.001	.001
			.045	.559	.032	.151	.014	.092	.084
0	.15	1.0	.037	.928	.033	.001	.001	.002	0
			.026	.631	.021	.134	.008	.090	.068
0	0	.1							
			.002	.001	.879	.001	.049	.053	.015
0	0	.4							
			.002	.001	.811	.001	.077	.075	.031
0	0	1.6	.154	.149	.653	.005	.018	.020	.000
			.057	.062	.720	.030	.046	.046	.005
0	0	2.8	.138	.145	.522	.020	.079	.083	.013
			.033	.032	.810	.021	.026	.029	.003
.2	.1	1.0	.408	.532	.050	.009	.001	.001	0
			.162	.219	.026	.395	.034	.040	.100
.4	.15	1.0	.589	.365	.019	.026	.001	0	0
			.255	.144	.020	.421	.030	.019	.087
.6	.15	1.0	.812	.149	.011	.027	.001	0	0
			.415	.061	.016	.366	.045	.007	.068
.8	.20	1.0	.817	.123	.007	.051	.001	0	0
			.412	.044	.016	.405	.035	.004	.060

From Table 6, we can see that for a single shift in the standard deviation, our proposed parametric test method is more effective, but for a single shift in the intercept or slope, the KMW chart actually performs better than our method. But our proposed approach has much better performance than the KMW chart in identifying the special cause in which there are simultaneous shifts in the intercept and slope, regardless of the shift sizes. In summary, using the hypothesis test method may alleviate the problem of the KMW chart in identifying multiple parameter changes, but to some extent at the expense of the accuracy when indeed only a single parameter (either Y-intercept or the slope) has shifted.

It is noteworthy that the foregoing multivariate F-test may not work equally well in all cases. For example, sometimes the explanatory variables of model (1) are highly correlated but contain the same predictive information. In such a case, we may find that the F-test statistics (14) corresponding to each of these variables may not be large enough to reject the null hypothesis, even if the underlying relationship have changed substantially. For this, we may consider applying multiple t-tests for the components of $\mathbf{DZ}_j$ mentioned in Section 4 individually. However, similar to the discussions in Section 4, it is not trivial to decide which matrix $\mathbf{D}$ should be used. In addition, the diagnostic results of using the foregoing test method is often difficult to interpret, because obtaining the corresponding practical meanings (either engineering or physical) of these independent components may not be easy.

As may be noted, the proposed test statistics do not really follow the given null distributions (t, F, or chi-squared) when the process is in control, because these statistics are obtained on the condition that the proposed MEWMA chart has triggered a signal and a changepoint estimate has been obtained. As one of the referees pointed out, this fact may not fundamentally change anything that we do in the diagnostic analysis, but it perhaps should affect the interpretation of the type I error. In addition, the effectiveness of such a testing method depends on the accuracy of the estimate of the changepoint. Moreover, when p is rather large, these $p + 1$ joint tests may not allow an accurate decision if we want to strictly control the overall type I error. Thus, although this testing diagnostic method can work well in most cases, engineers still may need to take the technical/engineering knowledge about the profile into consideration after obtaining guidance from the statistical diagnostic results.

8. ILLUSTRATION OF THE IMPLEMENTATION STEPS: THE DRIE MONITORING CASE REVISITED

Here we revisit the DRIE profile monitoring case presented in Section 2 and use that example to demonstrate how to implement the proposed scheme step by step in practice. Note that our proposed scheme may not be applied to the whole DRIE profile directly, because the whole profile cannot be readily viewed as a polynomial or a general linear model. In fact, the engineers indicate that the left and right corners of each profile contain sufficient information to distinguish the out-of-control conditions. Because these two sides usually present symmetric shapes, the engineers agree to choose the left corner to implement the control scheme [see Fig. 2(a)].

First, based on the same frame of reference for each profile, we find a reference point A according to a prescribed chosen coordinate, as shown in Figure 2(a). Then with A as original point, we rotate the left corner of the profile 45 degrees counterclockwise, as shown by Figures 2(b) and 2(c). The corner profile after rotation can then be adequately described by a quadratic polynomial model.

Here we collect dimensional readings by the SEM from 18 anisotropic profiles known to be in control. For each profile, we fix $x_i, i = 1, \ldots, 11$, which are equally spaced values, -2.5, (.5), 2.5. We can then obtain the following estimated IC model based on the readings of the corner profiles after rotation (the dataset is provided in the App.):

$$y_{ij} = ax_i^2 + \varepsilon_{ij}, \qquad i = 1, \ldots, n, \tag{15}$$

where $a = .62$ and $\sigma = .4$. This model is in the same form as model (1) with $\boldsymbol{\beta} = (\beta^{(1)}, \beta^{(2)}, \beta^{(3)}) = (1.55, 0, .62)$.

In practice, the change in regression coefficients $\boldsymbol{\beta}$ may indicate a positive or negative profile due to underetching or overetching. An increase in variation may correspond to a coarse profile or to greater inaccuracies in the etching process. A decrease in the variation of the curve would indicate an improvement in the etching process, as long as the regression coefficients do not change. With these insights, we then apply the proposed MEWMA scheme to monitor the quadratic profile and to detect whether there is any deviation in the process parameters. Detailed implementation steps are as follows.

Step 1. Choose the desired IC ARL and the smoothing constant, λ. Determine the control limit, L, based on p, IC ARL, and λ. Here $L = 15.41$ given that $p = 3$, ARL $= 370$, and $\lambda = .2$. Consequently, $L\sqrt{\frac{\lambda}{2-\lambda}}$ will be 1.71. Then we can construct the MEWMA control chart as in Figure 3.

Step 2. Start monitoring the process and obtain product observations y_{ij} at fixed values of x_i for $i = 1, \ldots, 11$, sequentially. Whenever obtaining a new sample, compute W_j. Consequently, compute the plot statistic, U_j, in (8) and compare it with control limit $L\sqrt{\frac{\lambda}{2-\lambda}}$. Because it is rather difficult and expensive to

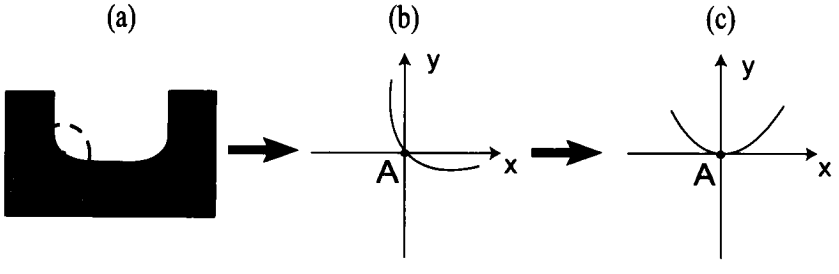

Figure 2. Modeling the DRIE profile.

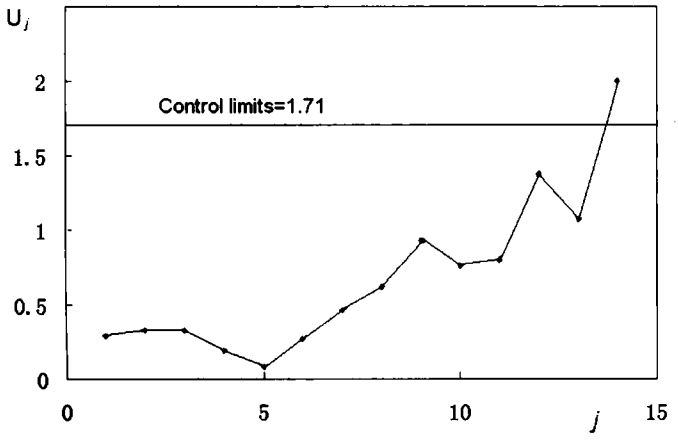

Figure 3. MEWMA chart for the example.

collect out-of-control sample profiles in the laboratory, in this example we artificially add a shift of $\beta^{(3)}$ on the IC model from .62 to .67 after the fifth sample and generate the OC profiles through Monte Carlo simulation. The simulated y_{ij} and corresponding U_j for $j = 1, \ldots, 14$ are tabulated in Table 7.

Figure 4 illustrates these IC and OC sample profiles in time sequence. After the fifth profile, the DRIE process starts to generate negative profiles that are considered defective. Note that the magnitudes of change in these profiles are usually slight and hard to distinguish by bare eyes in practice. This further motivates the need of an effective SPC monitoring scheme. From Table 7 and Figure 3, we can see that the MEWMA chart quickly signals such a shift at the 14th sample.

Step 3. By looking at the values of $lr(jn, 14n)$ for $j = 0, 1, \ldots, 13$, tabulated in the last column of Table 7, we see that its maximum occurs at $j = 5$ with $lr(5n, 14n) = 17.78$. This maximum precisely indicates the changepoint location, τ, of the shift.

Step 4. Finally, by computing the test statistics, T_{test}, χ^2_{test}, and $F^{(i)}_{test}$ for $i = 2, 3$ given in (12), (13), and (14), we obtain $T_{test} = -.427$, $\chi^2_{test} = 115.3$, $F^{(2)}_{test} = .019$, and $F^{(3)}_{test} = 13.4$. Considering a significant level, $\alpha = .05$, it follows that $|T_{test}| < |t(.025; 9n - 3)| = 1.985$ and $70.8 = \chi^2(.025; 9n - 3) < \chi^2_{test} < \chi^2(.975; 9n - 3) = 125.0$, $F^{(2)}_{test} < F_{.95}(2, 9n - 3, \mathbf{R}) = 3.94$, and $F^{(3)}_{test} > F_{.95}(2, 9n - 3, \mathbf{R}) = 3.94$, where $t(\alpha; \nu)$ and $\chi^2(\alpha; \nu)$ are the lower percentiles of the Student-t distribution and the chi-squared distribution with ν degrees of freedom. Thus our diagnosis concludes that there is a positive shift in the $\beta^{(3)}$ parameter [i.e., a in (15)] after sample 5. Figure 5 provides the time plot of the $\beta^{(3)}$ parameter estimate that also shows a slight change in this coefficient. Such an increase in the second-order coefficient of the profile indicates an unacceptable negative trend, which may be due to overetching, and the inductively coupled plasma machine settings and DRIE process conditions need to be reexamined.

Step 5. After correctly identifying the out-of-control parameters and fixing the problem, we then return to Step 1 to revise the design of the chart and restart the monitoring procedure for the DRIE process.

9. CONCLUSION

In this article we have proposed a complete solution to monitor a general linear profile that includes both a polynomial regression and a multiple linear regression model and can represent various industrial processes. We apply an MEWMA scheme to the transformations of estimated profile parameters as a single chart to monitor both the coefficients and variance of a general linear profile. The proposed scheme can easily be designed and constructed, and it has satisfactory performance. In particular, two additional features—the variable sampling interval and parametric diagnostic approach—are provided to enhance the efficiency and effectiveness of the proposed profile monitoring scheme. As demonstrated by the semiconductor DRIE case, the proposed monitoring scheme may be implemented in industrial practice as long as the quality of a process can be characterized by a general linear profile.

ACKNOWLEDGMENTS

The authors thank the editor, associate editor, and two anonymous referees for their helpful comments that have resulted

Table 7. Data for example with a shift in $\beta^{(3)}$ after the fifth sample

j	y_{ij}											U_j	lr
0													10.59
1	2.64	2.70	2.10	.35	.32	.35	.94	.31	1.15	2.70	4.09	.29	13.15
2	4.60	2.51	1.28	.94	−.09	−.29	.96	.82	1.38	1.66	3.57	.33	14.43
3	4.21	2.09	1.36	1.18	.34	−.67	.54	−.03	1.51	2.82	3.70	.33	14.92
4	3.11	2.46	1.59	.46	−.45	.44	.05	.49	1.71	2.79	4.06	.19	17.07
5	4.14	2.19	1.08	.47	.29	−.08	.00	.80	1.05	3.02	4.00	.08	**17.78**
6	3.64	2.87	.25	.51	.24	.37	−.53	.61	1.40	2.35	4.31	.27	17.65
7	4.40	2.58	1.25	.41	.13	.19	−.31	−.09	1.15	3.42	4.07	.46	14.09
8	3.92	2.78	1.74	.10	.61	−.99	−.02	.30	2.05	2.56	3.61	.62	13.03
9	4.66	2.97	1.50	1.06	.12	−.48	−.54	.48	1.21	3.01	3.73	.93	9.15
10	4.34	2.27	1.31	.52	.19	−.10	.14	1.07	1.04	3.02	3.86	.76	11.11
11	3.89	1.82	1.31	.08	−.11	.49	−.18	−.28	1.68	2.62	4.12	.80	11.12
12	4.52	2.43	1.50	.46	−.38	−.61	.01	1.32	1.20	2.71	4.42	1.38	9.67
13	3.53	2.59	2.57	.26	.01	.13	.12	.43	2.02	2.39	4.20	1.07	14.15
14	4.42	3.02	1.93	−.37	.30	−.95	−.65	1.14	.76	1.55	3.93	**2.00**	

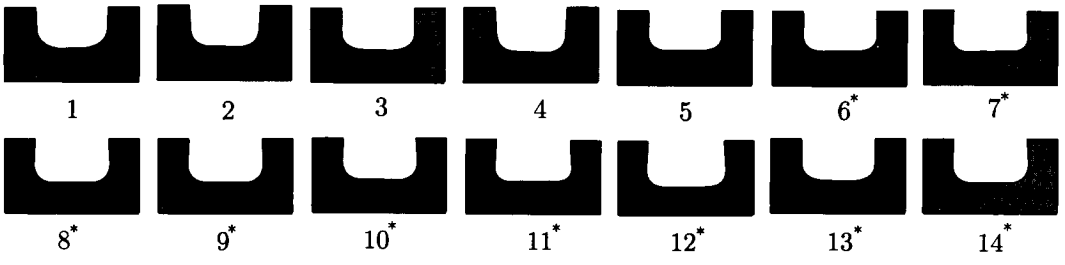

Figure 4. Illustrations of 14 sample profiles. The symbol "*" in the exponent of sample number represents an OC profile.

in significant improvements in the article. This work was completed when Zou was a research assistant at the Hong Kong University of Science and Technology, whose hospitality is appreciated and acknowledged. This research was supported by RGC Competitive Earmarked Research grants HKUST6232/04E and HKUST6204/05E. Zou and Wang also thank the support of the Natural Sciences Foundation of Tianjin.

APPENDIX A: ARL AND ATS CALIBRATIONS OF THE PROPOSED PROFILE MONITORING SCHEME

Because our proposed chart is a special case of the MEWMA chart proposed by Lowry et al. (1992), the Markov chain approximation presented by Runger and Prabhu (1996) may be extended to calculate our ARLs. Here we briefly describe the Markov chain approximation method, but highlight some necessary modifications. (For more details on the Markov chain approximation for a conventional MEWMA chart, see Runger and Prabhu 1996.)

First, because the vector $\mathbf{Z}$ (here we suppress the sample number j for simplicity) is a normal vector with mean $\mathbf{0}$ and covariance matrix $\mathbf{\Sigma}$, the IC ARL can be evaluated by the same approach as taken by Runger and Prabhu (1996). A one-dimensional Markov chain is used to approximate the IC ARL. Define the $(m+1) \times (m+1)$ transition probability matrix, $\mathbf{P} = (p_{ij})$, where the element p_{ij} denotes the probability of a transition from state i to j and $(m+1)$ is the number of transition states. Now, we have for $i = 0, 1, 2, \ldots, m$,

$$p_{ij} = f_1^{-1}\left((j+0.5)^2 g^2/\lambda^2; p+1; \xi\right) - f^{-1}\left((j-.5)^2 g^2/\lambda^2; p+1; \xi\right), \qquad 0 < j \le m$$

and

$$p_{i0} = f_1^{-1}\left((.5)^2 g^2/\lambda^2; p+1; \xi\right), \qquad j = 0,$$

where $g = (L\frac{\lambda}{2-\lambda})^{1/2}/(m+1)$, $\xi = [(1-\lambda)ig/\lambda]^2$, and $f_1^{-1}(\cdot; \nu; \xi)$ is the inverse function of the noncentral chi-squared distribution function with ν degrees of freedom and noncentrality parameter ξ. Then the IC ARL can be evaluated by

$$\mathrm{ARL} = \mathbf{l}'(\mathbf{I} - \mathbf{P})^{-1}\mathbf{1},$$

where $\mathbf{I}$ denotes the $(m+1)$-dimensional identity matrix and $\mathbf{l}$ is a $(m+1)$ vector with a 1 as the first element. Note that the computer program, which calculates the ARL of the MEWMA chart presented by Molnau et al. (2001), can be directly utilized.

Next we consider the approximation under an out-of-control condition. Lowry et al. (1992) and Runger and Prabhu (1996) have shown that the off-target performance of the MEWMA chart may be determined by assuming, without loss of generality, that the off-target mean vector is $\delta\mathbf{I}$. The two-dimensional Markov chain can then be used to analyze the OC ARL of MEWMA. One dimension that includes $m_2 + 1$ states is used to analyze the properties of IC components, whereas the other dimension of the Markov chain that has $2m_1 + 1$ transition states is used to analyze the performance of the OC component. Therefore, a $(2m_1 + 1) \times (m_2 + 1)$-dimensional matrix is used.

In our case, when the regression coefficients of a linear profile change, i.e., from $\boldsymbol{\beta}$ to $\boldsymbol{\beta}^*$, the noncentrality parameter, δ, is

$$\delta = \frac{1}{\sigma}\sqrt{(\boldsymbol{\beta}^* - \boldsymbol{\beta})'(\mathbf{X}'\mathbf{X})(\boldsymbol{\beta}^* - \boldsymbol{\beta})}. \qquad \text{(A.1)}$$

However, when the standard deviation of the profile changes from σ to $\delta\sigma$, both the distributions of $\mathbf{Z}(\boldsymbol{\beta})$ and $Z(\sigma)$ also will change, although their independency still holds. Furthermore, the $Z(\sigma)$ no longer will be normally distributed. Thus some modifications are needed to obtain the OC ARL in the profile case.

In fact, if we divide $\mathbf{Z}$ by δ, the distributions of $\mathbf{Z}(\boldsymbol{\beta})$ will be a p-dimensional vector that was standard multivariate normally distributed. It can be verified that the run-length distributions of the EWMA of $\mathbf{Z}/\delta$ with the control limit $L\frac{\lambda}{2-\lambda}/\delta$ turn out to be the same as that of the EWMA of $\mathbf{Z}$ with the control limit $L\frac{\lambda}{2-\lambda}$;

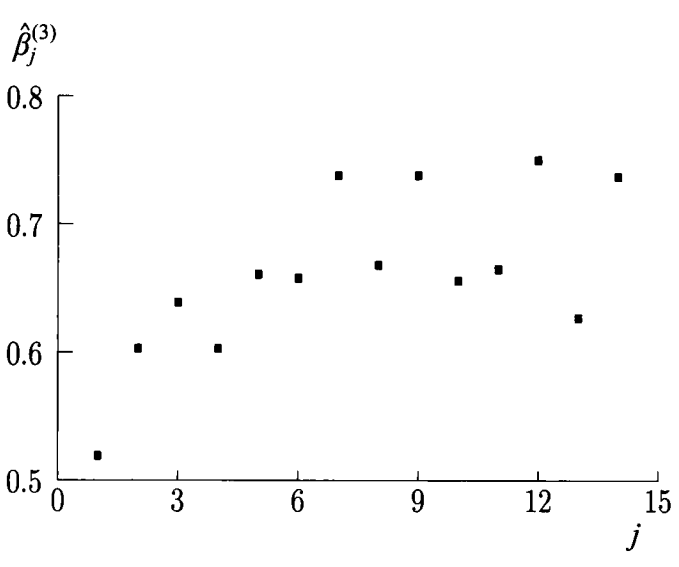

Figure 5. Time plot of the $\beta^{(3)}$ parameter estimate.

thus a two-dimensional Markov chain still can be used for this case. The on-target one-dimensional Markov chain can then be obtained through a similar approach as for the IC case described above with the control limits $L\frac{\lambda}{2-\lambda}/\delta$ replacing $L\frac{\lambda}{2-\lambda}$, and degrees of freedom $p+1$ replacing p in the f_1^{-1} function. Moreover, the transitional probability of the off-target part, $Z(\sigma)/\delta$, from state i to j denoted by $v(i,j)$ can be obtained as follows. Similar to Runger and Prabhu (1996), we partition the control limits, $-L\frac{\lambda}{2-\lambda}/\delta$ and $L\frac{\lambda}{2-\lambda}/\delta$, into $2m+1$ states of length g. Let $c_i = -L\frac{\lambda}{2-\lambda}/\delta + (i-.5)g$. Then,

$$\begin{aligned} v(i,j) &= \Pr\left\{\frac{1}{\lambda}\left[-L\frac{\lambda}{2-\lambda}\Big/\delta + (j-1)g - (1-\lambda)c_i\right]\right. \\ &\quad \left. < \frac{Z(\sigma)}{\delta} < \frac{1}{\lambda}\left[-L\frac{\lambda}{2-\lambda}\Big/\delta + jg - (1-\lambda)c_i\right]\right\} \\ &= F\left(F^{-1}\left(\Phi\left(\frac{\delta}{\lambda}\left[-L\frac{\lambda}{2-\lambda}\Big/\delta + jg - (1-\lambda)c_i\right]\right); \right.\right. \\ &\quad \left.\left. n-p\right)\delta^2\Big/; n-p\right) \\ &\quad - F\left(F^{-1}\left(\Phi\left(\frac{\delta}{\lambda}\left[-L\frac{\lambda}{2-\lambda}\Big/\delta + (j-1)g\right.\right.\right. \\ &\quad \left.\left.\left. - (1-\lambda)c_i\right]\right); n-p\right)\Big/\delta^2; n-p\right), \end{aligned}$$

where F is the chi-squared distribution function defined in Section 3. After that, we combine the two one-dimensional transition probability matrices into a bivariate Markov chain by the methodology of Runger and Prabhu (1996). The OC ARL when a shift in the standard deviation occurs then can be obtained.

Now we consider the calculation of the ATS and SSATS for profile monitoring. When the process is in control, we can obtain a one-dimensional transition probability matrix, $\mathbf{P}$, from the calculation of the ARL for the MEWMA chart. Using the same methodology as in Reynolds et al. (1990), the IC ATS can be expressed as

$$\text{ATS} = d_0 + \mathbf{l}'(\mathbf{I}-\mathbf{P})^{-1}\mathbf{d},$$

where d_0 is the interval between the beginning of the process and the time when the first sample is taken and $\mathbf{d}$ is a $(m+1)$ vector. The ith element of $\mathbf{d}$ corresponds to the interval to be taken after the control statistics fall inside the state, i. The approach to determine the $\mathbf{d}$ is as follows. When the upper limit of ith state is smaller than the warning limit, say $(i+.5)g \le (L_1\frac{\lambda}{2-\lambda})^{1/2}$, then the ith element of $\mathbf{d}$ is d_2. When the lower limit of the ith state is larger than the warning limit, say $(i-.5)g > (L_1\frac{\lambda}{2-\lambda})^{1/2}$, then the ith element of $\mathbf{d}$ is d_1. When the warning limit falls between the upper limit and lower limit, the extrapolations are used. In this article, all of the numerical results are for the general case with $d_0 = 1$.

To compute the SSATS, the bivariate Markov chain illustrated earlier can be applied as well. Note that although the two-dimensional Markov chain is used to determine the statistical properties of the MEWMA chart when the process is out of control, it is also be valid in the in-control case. Define $\mathbf{Q}_0$ as the $(2m_1+1)\times(m_2+1)$-dimensional transition probability matrix when the process is in control. Let $\mathbf{d}$ be a $(2m_1+1)\times(m_2+1)$ vector; the ith element of this vector corresponds to the interval being taken after the control statistics fall inside the state, i. Denote $\boldsymbol{\pi}$ to be the normalized eigenvector subject to $\boldsymbol{\pi}'\mathbf{Q}_0 = \boldsymbol{\pi}'$. Suppose that $\boldsymbol{\alpha}$ is the vector of starting probabilities that the shift occurs in an interval between samples. Then $\boldsymbol{\alpha}$ can be expressed in matrix notation, $\boldsymbol{\alpha}' = \frac{\boldsymbol{\pi}'\mathbf{D}}{\boldsymbol{\pi}'\mathbf{d}}$, where $\mathbf{D}$ is a diagonal matrix with $\mathbf{d}$ on the diagonal. Then the SSATS can be expressed as

$$\text{SSATS} = \boldsymbol{\alpha}'\left[(\mathbf{I}-\mathbf{Q})^{-1} - \frac{1}{2}\mathbf{I}\right]\mathbf{d},$$

where $\mathbf{Q}$ is a $(2m_1+1)\times(m_2+1)$ dimension matrix when the process is out of control. The $\mathbf{Q}$ can then be calculated by the same method used to calculate the OC ARLs. In addition, similar to Runger and Prabhu (1996), we compute $(\mathbf{I}-\mathbf{P})\mathbf{b} = \mathbf{1}$, which can be quicker than computing $(\mathbf{I}-\mathbf{P})^{-1}\mathbf{1}$ directly when obtaining the ARL and ATS.

In this article we obtain the IC ARL and ATS using $m = 100$ and obtain the OC ARL and SSATS using $m_1 = m_2 = 30$.

We have conducted simulations to verify the accuracy of the Markov chain approximation for the profile monitoring case, and the results are very satisfactory.

APPENDIX B: THE EXPRESSION OF *lr*(*tn*, *kn*)

Based on the changepoint model, Mahmoud et al. (2007) gave a likelihood ratio test (LRT) statistic for linear profiles in phase I. This LRT statistic is similar to that of Quandt (1958) and is derived under the assumption that the parameters of the null hypothesis are unknown. Thus it is not appropriate in phase II that the in-control parameters are assumed known. After k samples have been collected, the logarithm of the likelihood function for them is given by

$$-\frac{1}{2}\sum_{j=1}^{k}\left[n\ln(2\pi\sigma_j^2) + \frac{1}{\sigma_j^2}(\mathbf{Y}_j - \mathbf{X}\boldsymbol{\beta}_j)'(\mathbf{Y}_j - \mathbf{X}\boldsymbol{\beta}_j)\right].$$

If the data are collected under in-control conditions (i.e., under the null hypothesis), then the value of the logarithm of the likelihood function is

$$l_0 = -\frac{1}{2}\sum_{j=1}^{k}\left[n\ln(2\pi\sigma^2) + \frac{1}{\sigma^2}(\mathbf{Y}_j - \mathbf{X}\boldsymbol{\beta})'(\mathbf{Y}_j - \mathbf{X}\boldsymbol{\beta})\right].$$

Assuming that a shift occurs after t, the corresponding maximum value of the logarithm of likelihood is

$$\begin{aligned} l_1 = &-\frac{1}{2}\sum_{j=1}^{t}\left[n\ln(2\pi\sigma^2) + \frac{1}{\sigma^2}(\mathbf{Y}_j - \mathbf{X}\boldsymbol{\beta})'(\mathbf{Y}_j - \mathbf{X}\boldsymbol{\beta})\right] \\ &- \frac{(k-t)n}{2}\ln\left(2\pi\tilde{\sigma}_{(t,k)}^2\right) - \frac{(k-t)n}{2}, \end{aligned}$$

where $\tilde{\sigma}_{(t,k)}^2 = \frac{(k-t)n-p}{(k-t)n}\tilde{\sigma}_{t,k}^2$ and $\tilde{\sigma}_{t,k}^2$ is as defined in (11).

Then the generalized likelihood ratio statistic is given by

$$lr(tn, kn) = -2(l_0 - l_1)$$

$$= \sum_{j=t+1}^{k} \frac{1}{\sigma^2}(\mathbf{Y}_j - \mathbf{X}\boldsymbol{\beta})'(\mathbf{Y}_j - \mathbf{X}\boldsymbol{\beta})$$

$$- (k-t)n\left[\ln\left(\frac{\tilde{\sigma}^2_{(t,k)}}{\sigma^2}\right) + 1\right].$$

APPENDIX C: DATASET OF 18 IN-CONTROL ANISOTROPIC PROFILES

Readings y of corner profiles after rotation by SEM

j	y_{ij} (unit: μm)										
1	3.47	1.95	1.43	.38	−.20	−.32	.20	.57	1.50	2.64	4.02
2	3.92	2.16	1.53	.03	.15	−.22	.70	.62	1.16	1.68	3.98
3	4.04	2.68	1.10	.51	.26	.17	−.56	.92	1.15	1.69	3.71
4	3.76	2.54	1.91	1.21	−.07	−.09	.06	.63	1.77	2.26	4.05
5	2.75	2.82	1.26	.92	.11	−.71	−.02	1.39	1.14	1.80	3.75
6	3.60	3.00	1.02	.55	−.09	1.24	−.10	.53	1.51	2.20	4.28
7	3.70	1.55	1.51	.48	−.95	−.37	−.18	.47	1.65	2.56	3.91
8	3.69	2.78	.30	.53	.93	−.10	.62	1.00	1.68	2.62	4.05
9	3.94	3.31	2.21	.11	.50	−.84	.13	.90	1.30	2.42	3.55
10	3.72	3.01	.96	.40	−.27	.75	.07	.27	1.36	2.46	3.72
11	3.97	2.89	1.61	.68	.52	.36	−.45	.46	.80	1.99	3.25
12	3.89	2.12	1.15	.94	.13	.09	−.01	.68	1.77	2.83	4.26
13	4.23	2.34	1.32	.72	.13	.68	1.02	.03	1.35	3.20	4.34
14	3.95	2.20	1.02	.78	.64	.52	.01	.83	1.23	2.39	3.72
15	4.28	2.97	1.41	.48	.49	−.84	−.07	.26	1.09	3.06	4.08
16	4.18	3.23	1.74	.70	.31	.53	−.36	.58	1.38	2.73	4.32
17	4.35	2.44	1.61	.84	1.21	.30	.49	1.30	1.31	2.14	4.01
18	3.19	2.71	1.20	.57	.31	−.51	.49	.75	1.78	1.53	4.30

[Received April 2006. Revised September 2006.]

REFERENCES

Aparisi, F. (2001), "Hotelling's T^2 Control Chart With Variable Sampling Intervals," *International Journal of Production Research*, 39, 3127–3140.

Calzada, M. E., Scariano, S. M., and Chen, G. (2004), "Computing Average Run Lengths for the MaxEWMA Chart," *Communications in Statistics, Part B—Simulation and Computation*, 33, 489–503.

Chen, G., Cheng, S. W., and Xie, H. (2001), "Monitoring Process Mean and Variability With One EWMA Chart," *Journal of Quality Technology*, 33, 223–233.

Chengular, I. N., Arnold, J. C., and Reynolds, M. R. Jr. (1989), "Variable Sampling Interval for Multiparameter Shewhart Charts," *Communications in Statistics, Part A—Theory and Methods*, 18, 1769–1792.

Croarkin, C., and Varner, R. (1982), "Measurement Assurance for Dimensional Measurements on Integrated-Circuit Photomasks," NBS Technical Note 1164, U.S. Department of Commerce.

Csorgo, M., and Horvath, L. (1997), *Limit Theorems in Change-Point Analysis*, New York: Wiley.

Gan, F. F. (1995), "Joint Monitoring of Process Mean and Variance Using Exponentially Weighted Moving Average Control Charts," *Technometrics*, 37, 446–453.

Gupta, S., Montgomery, D. C., and Woodall, W. H. (2006), "Performance Evaluation of Two Methods for Online Monitoring of Linear Calibration Profiles," *International Journal of Production Research*, 44, 1927–1942.

Hawkins, D. M., and Zamba, K. D. (2005), "Statistical Process Control for Shifts in Mean or Variance Using a Change-Point Formulation," *Technometrics*, 47, 164–173.

Jensen, D. R., Hui, Y. V., and Ghare, P. M. (1984), "Monitoring an Input–Output Model for Production. I: The Control Charts," *Management Science*, 30, 1197–1206.

Kang, L., and Albin, S. L. (2000), "On-Line Monitoring When the Process Yields a Linear Profile," *Journal of Quality Technology*, 32, 418–426.

Kim, K., Mahmoud, M. A., and Woodall, W. H. (2003), "On the Monitoring of Linear Profiles," *Journal of Quality Technology*, 35, 317–328.

Kotz, S., Balakrishnan, N., and Johnson, N. L. (2000), *Continuous Multivariate Distributions* (2nd ed.), New York: Wiley-Interscience.

Lawless, J. F., Mackay, R. J., and Robinson, J. A. (1999), "Analysis of Variation Transmission in Manufacturing Processes, Part I," *Journal of Quality Technology*, 31, 131–142.

Lowry, C. A., Woodall, W. H., Champ, C. W., and Rigdon, S. E. (1992), "Multivariate Exponentially Weighted Moving Average Control Chart," *Technometrics*, 34, 46–53.

Lucas, J. M., and Saccucci, M. S. (1990), "Exponentially Weighted Moving Average Control Scheme Properties and Enhancements," *Technometrics*, 32, 1–29.

Mahmoud, M. A., and Woodall, W. H. (2004), "Phase I Analysis of Linear Profiles With Calibration Applications," *Technometrics*, 46, 380–391.

Mahmoud, M. A., Parker, P. A., Woodall, W. H., and Hawkins, D. M. (2007), "A Change Point Method for Linear Profile Data," *Quality and Reliability Engineering International*, 23, 247–268.

May, G. S., Huang, J., and Spanos, C. J. (1991), "Statistical Experimental Design in Plasma Etch Modeling," *IEEE Transactions on Semiconductor Manufacturing*, 4, 83–98.

McAuley, S. A., Ashraf, H., Atabo, L., Chambers, A., Hall, S., Hopkins, J., and Nicholls, G. (2001), "Silicon Micromachining Using a High-Density Plasma Source," *Journal of Physics D-Applied Physics*, 34, 2769–2774.

Mestek, O., Pavlik, J., and Suchanek, M. (1994), "Multivariate Control Charts: Control Charts for Calibration Curves," *Journal of Analytical Chemistry*, 350, 344–351.

Molnau, W. E., Runger, G. C., Montgomery, D. C., Skinner, K. R., Loredo, E. N., and Prabhu, S. S. (2001), "A Program for ARL Calculation for Multivariate EWMA Charts," *Journal of Quality Technology*, 33, 515–521.

Nishina, K. (1992), "A Comparison of Control Charts From the Viewpoint of Change-Point Estimation," *Quality and Reliability Engineering International*, 8, 537–541.

Pignatiello, J. J. Jr., and Samuel, T. R. (2001), "Estimation of the Change Point of a Normal Process Mean in SPC Applications," *Journal of Quality Technology*, 33, 82–95.

Prabhu, S. S., and Runger, G. C. (1997), "Designing a Multivariate EWMA Control Chart," *Journal of Quality Technology*, 29, 8–15.

Quandt, R. E. (1958), "The Testing of the Parameters of a Linear Regression System Obeys Two Separate Regimes," *Journal of the American Statistical Association*, 53, 873–880.

Quesenberry, C. P. (1995), "On Properties of Q Charts for Variables," *Journal of Quality Technology*, 27, 184–203.

Rauf, S., Dauksher, W. J., Clemens, S. B., and Smith, K. H. (2002), "Model for a Multiple-Step Deep Si Etch Process," *Journal of Vacuum Science and Technology A*, 20, 1177–1190.

Reynolds, M. R. Jr. (1989), "Optimal Variable Sampling Interval Control Charts," *Sequential Analysis*, 8, 361–379.

Reynolds, M. R. Jr., and Arnold, J. C. (2001), "EWMA Control Charts With Variable Sample Sizes and Variable Sampling Intervals," *IIE Transactions*, 33, 66–81.

Reynolds, M. R. Jr., and Kim, K. (2005a), "Multivariate Monitoring of the Process Mean Vector With Sequential Sampling," *Journal of Quality Technology*, 37, 149–162.

——— (2005b), "Monitoring Using an MEWMA Control Chart With Unequal Sample Sizes," *Journal of Quality Technology*, 37, 267–281.

Reynolds, M. R. Jr., and Stoumbos, Z. G. (2001), "Monitoring the Process Mean and Variance Using Individual Observations and Variable Sampling Intervals," *Journal of Quality Technology*, 33, 181–205.

——— (2005), "Should Exponentially Weighted Moving Average and Cumulative Sum Charts Be Used With Shewhart Limits?" *Technometrics*, 47, 409–424.

Reynolds, M. R. Jr., Amin, R. W., and Arnold, J. C. (1990), "CUSUM Charts With Variable Sampling Intervals," *Technometrics*, 32, 371–384.

Reynolds, M. R. Jr., Amin, R. W., Arnold, J. C., and Nachlas, J. A. (1988), "$\bar{X}$ Charts With Variable Sampling Intervals," *Technometrics*, 30, 181–192.

Rigdon, S. E. (1995a), "A Double-Integral Equation for the Average Run Length of a Multivariate Exponentially Weighted Moving Average Control Chart," *Statistics and Probability Letters*, 24, 365–373.

——— (1995b), "An Integral Equation for the In-Control Average Run Length of a Multivariate Exponentially Weighted Moving Average Control Chart," *Journal of Statistical Computation and Simulation*, 52, 351–365.

Runger, G. C., and Montgomery, D. C. (1993), "Adaptive Sampling Enhancements for Shewhart Control Charts," *IIE Transactions*, 25, 41–51.

Runger, G. C., and Prabhu, S. S. (1996), "A Markov Chain Model for the Multivariate Exponentially Weighted Moving Averages Control Chart," *Journal of the American Statistical Association*, 91, 1701–1706.

Stover, F. S., and Brill, R. V. (1998), "Statistical Quality Control Applied to Ion Chromatography Calibrations," *Journal of Chromatography A*, 804, 37–43.

Woodall, W. H., Spitzner, D. J., Montgomery, D. C., and Gupta, S. (2004), "Using Control Charts to Monitor Process and Product Quality Profiles," *Journal of Quality Technology*, 36, 309–320.

Zhou, R., Zhang, H., Hao, Y., and Wang, Y. (2004), "Simulation of the Bosch Process With a String-Cell Hybrid Method," *Journal of Micromechanics and Microengineering*, 14, 851–858.

Zou, C., Zhang, Y., and Wang, Z. (2006), "Control Chart Based on Change-Point Model for Monitoring Linear Profiles," *IIE Transactions*, 38, 1093–1103.